Supporting Information

Wang *et al*. 10.1073/pnas.0804871105

SI Materials and Methods

Cell Culture and Transfection. Human neuroblastoma M17 cells were grown as described before (1). Transfection was performed using Effectene (Qiagen) (2); 300 μg/ml geneticin (Invitrogen) or 400 μg/ml of hygromycin B (Calbiochem) was included in the medium for stable cell line selection. Stable cell lines were maintained with 100 μg/ml geneticin or 200 μg/ml of hygromycin.

Antibodies. Primary antibodies used included mouse anti-DLP1/OPA1 (BD), mouse anti-Mfn1 (Novus Biologicals), mouse anti-Mfn2 (Sigma), rabbit anti-Fis1 (Imgenex), mouse anti-APP (6E10, Signet), rabbit anti-α-tubulin (Epitomics) and mouse anti-α-tubulin/Myc (Cell Signaling).

Expression Vectors. Mito-DsRed2 (Clontech), APPwt and APPswe constructs (gift from Huaxi Xu, The Burnham Institute) were obtained. Mito-AcGFP was constructed by replacing DsRed2 with AcGFP (cDNA from Clontech) based on the Mito-DsRed2 vector. The expression plasmids for DsRed-Monomer tagged APPwt or APPswe were constructed based on pDsRed-Monomermer-N1 Vector (Clontech). The expression plasmids for myc tagged wild type DLP1 (cDNA gift from Yisang Yoon, University of Rochester), myc tagged wild type OPA1 (cDNA gift from Luca Scorrano, Venetian Institute of Molecular Medicine, Italy) were constructed based on pCMV-Tag3 Vector (Stratagene). Dendra2 (Evrogen) is a commercial updated version of Dendra, a compound which readily changes from green to red fluorescent states when photoconverted by 400nm or 490nm light. We constructed mito-Dendra2 (based on pCMV vector from Clontech) containing a cleavable N-terminal mitochondrial targeting sequence from subunit VIII of cytochrome c oxidase (COXVIII) to drive Dendra2 specifically into the mitochondria matrix. By cotransfection with Mito-DsRed2, the specific localization of mito-Dendra2 in mitochondria was confirmed.

Cell Treatments and Measurements. Cells were seeded at low density on 6-well plates or in 4-well chamber slides and cultured for 24 h before treatments with β-secretase inhibitor IV (Calbiochem) in normal growth media. Treatments lasted 4 days at a concentration of 20 nM. ADDLs was prepared using $A\beta_{1-42}$ peptide (California Peptide, Napa, CA), as described (3), except that phenol red free neurobasal medium (Invitrogen) was used. As a control, $A\beta_{42-1}$ was subject to the same procedure before applying to cells. Primary hippocampal cells were usually transfected at DIV7 and treated with ADDLs 2 days after transfection. Cytotoxicity was measured by Cytotoxicity Detection Kit (LDH; Roche). $A\beta_{1-42}$ level was determined by $A\beta$ [1–42] ELISA KIT (Invitrogen). To differentiate M17 cells, serum content was reduced to 2% and 1 μM retinoic acid (Sigma-Aldrich) was included in the culture media. ATP levels were measured by the ATP Determination Kit, ROS by H_2DCFDA, MMP by Rhodamine 123 (Rh123) and MMP-independent dye Mitotracker Red 580 FM according to manufacturer's instructions (all from Invitrogen).

Western blot analysis, electron microscopy, and immunofluorescence were performed as described (2).

Hippocampal Neuron Culture and Transfection. Primary neurons from E18 rat hippocampus (BrainBits) were seeded at 30,000–40,000 cells per well on 8-well chamber slides coated with Poly-D-Lysine/Laminin (BD) in neurobasal medium supplemented with 2% B27 (Invitrogen)/0.5 mM glutamine/25 mM glutamate. Half the culture medium was changed every 3 d with neurobasal medium supplemented with 2% B27 (Invitrogen) and 0.5 mM glutamine. All cultures were kept at 37°C in a humidified 5% CO2 containing atmosphere. More than 90% cells were neurons after they were cultured for 7 days in vitro (DIV), verified by positive staining for neuronal specific markers microtubule-associated protein-2 (MAP2, dendritic marker) and Tau-1 (axonal marker). At DIV7, neurons were transfect using Neurofect (Genlantis) according to manufacturer's protocol.

Mitochondria Isolation. Mitochondria in M17 cells were isolated similarly as described before (4). Briefly, M17 cells were washed two times with Dulbecco's Phosphate-Buffered Saline (D-PBS, Invitrogen), and resuspended in ice cold permeabilization buffer containing 200 mM mannitol, 70 mM sucrose, 1 mM EGTA, 10 mM Hepes, 1 mM PMSF and protease inhibitor cocktail (Sigma). Cells were homogenized on ice with a 1-cc insulin syringe 27G1/2, drawing through the needle 20 times. Following centrifugation at 600 $\times g$ at 4°C for 20 min, the supernatant was collected, and centrifuged at 8,000 $\times g$ at 4°C for 15 min. The supernatant containing cytoplasmic proteins was stored at -20°C. The pellet was washed two times with permeabilization buffer. Finally, mitochondria were lysed with 1 $\times$ Cell Lysis Buffer (Cell Signaling), plus 1 mM PMSF (Sigma) and protease inhibitor cocktail (Sigma).

Time-Lapse Imaging. Cells were seeded in glass-bottomed dishes (MatTek) and transfected with Mito-Dendra2. 48 h after transfection, cells were put in a well-equipped live imaging station (Zeiss CTI-Controller 3700) with controlled CO_2 content, humidity and temperature of stage, objective and the air. Images were captured with a Zeiss LSM 510 inverted laser-scanning confocal fluorescence microscope. Images of red signal were collected using 543-nm excitation light from an argon laser and a 560-nm long pass filter; green fluorescence was collected using 488-nm excitation light from an argon laser and a 500- to 550-nm band-pass barrier filter. Fast and sufficient photoswitch of Mito-dendra2 was achieved by exposing highly zoomed area to 1% 488-nm laser intensity for 7 iterations. During time-lapse imaging, frames were captured every 10s for at least 1h without apparent phototoxicity or photobleaching. Image analysis was also performed with open-source image-analysis programs WCIF ImageJ (developed by W. Rasband) and Image-Pro Plus 6.0 (Media Cybernetics).

1. Zhu X, *et al.* (2004) Neuroprotective properties of Bcl-w in Alzheimer disease. *J Neurochem* 89:1233–1240.
2. Wang X, Su B, Fujioka H, Zhu X (2008) Dynamin-like protein 1 reduction underlies mitochondrial morphology and distribution abnormalities in fibroblasts from sporadic Alzheimer's disease patients. *Am J Pathol* 173:470–482.
3. Klein WL (2002) Abeta toxicity in Alzheimer's disease: Globular oligomers (ADDLs) as new vaccine and drug targets. *Neurochem Int* 41:345–352.
4. Frezza C, Cipolat S, Scorrano L (2007) Organelle isolation: functional mitochondria from mouse liver, muscle and cultured fibroblasts. *Nat Protocols* 2:287–295.

Fig. S1. (*A*) A boundary line linking all of the mitochondria at the edge was drawn (*Inset*) to encircle an area containing all mitochondria within the cell. The size of the cytoplasmic area outside this circled area was measured and its percentage of the entire cytoplasmic area was calculated. This was termed the cytoplasmic area devoid of mitochondria. The cytoplasmic area devoid of mitochondria in 1,000 cells per line was determined and compared between vector-control and APP-overexpressing cells. The shaded boxes contain 95% of the values for each condition, with the dashed line representing the mean and the solid line representing the median value. The dots show the range of values obtained and the error bars represent SEM. Ninety-five percent of control M17 contained between 0.08% and 3.38% cytosolic area covered by mitochondria (i.e., shaded box), with a mean value of 1.6%. However, APPwt or APPswe cells were significantly different, i.e., 95% of APPwt cells containing between 0.08% and 12.56% cytosolic area covered by mitochondria, with a mean of 7.43%, and 95% of APPswe cells containing between 20.39% and 34.3% cytosolic area covered by mitochondria, with a mean of 27.45%. Based on these data, the cell was classified as having an abnormal mitochondrial distribution if at least 10% of the cytosolic area was devoid of mitochondria. If more than 90% of the cytosolic area was covered by mitochondria, the cell was classified with normal mitochondrial distribution. $*P < 0.05$, Student *t* test. (*B*) Representative confocal microscopic images show three types of mitochondria morphology (normal tubular, fragmented, and elongated form).

Fig. S2. EM analysis of mitochondrial distribution and morphology. Representative micrographs of controls (*A*, *A′*), APPwt (*B*, *B′*) and APPswe (*C*, *C′*) M17 cells were shown. *A′*, *B′*, *C′* were larger magnification of the areas highlighted in *A*–*C*. n, nucleus; solid lines, cell border; dotted lines, mitochondria-containing area; asterisks, damaged mitochondria. (*D*) Total mitochondrial number is reduced but number of damaged mitochondria increased in APPwt and APPswe M17 cells. *, $P < 0.05$. (*E*) Mitochondria size and width increased, but length decreased significantly in APPwt or APPswe M17 cells ($P < 0.05$).

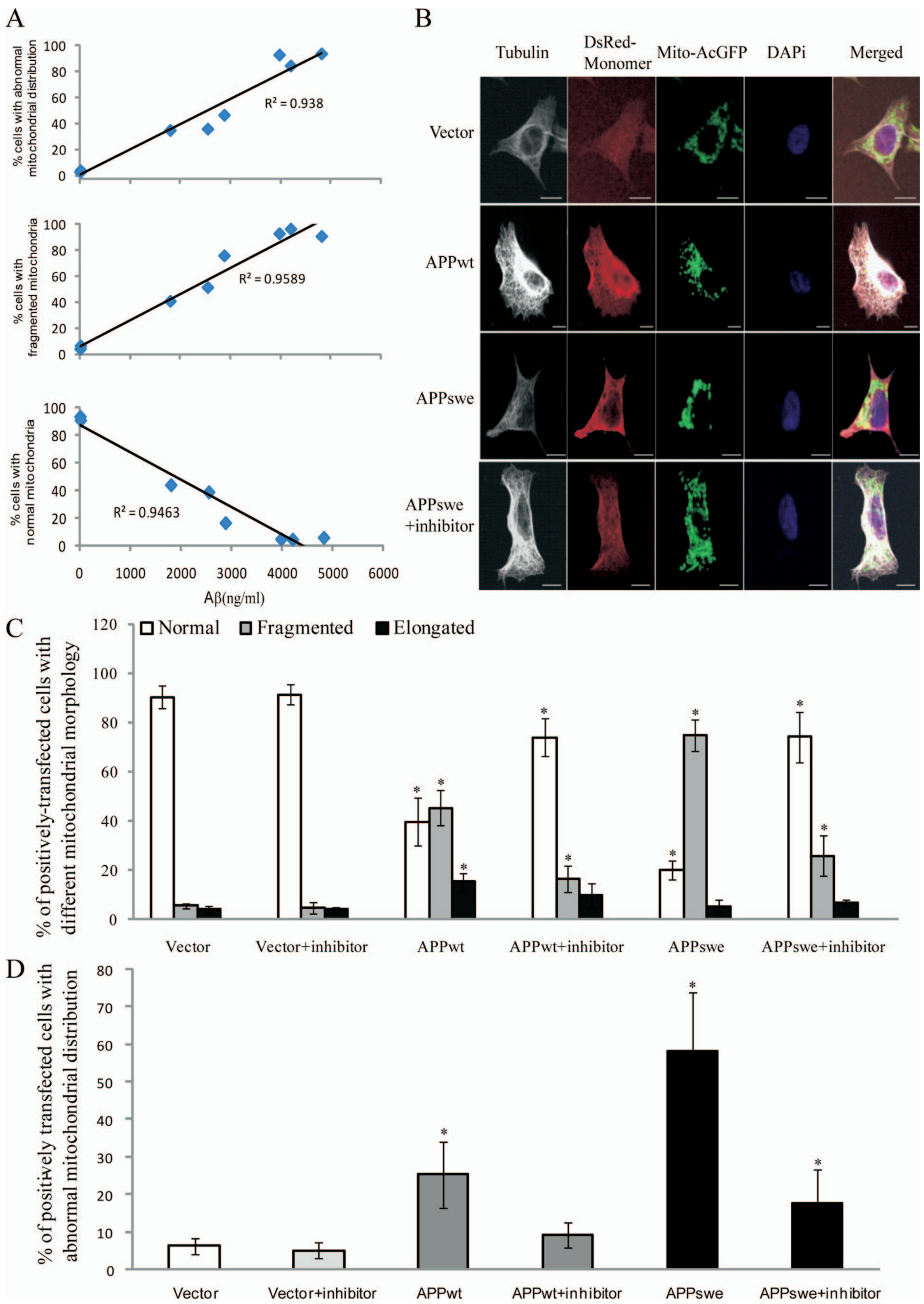

Fig. S3. (*A*) Quantification reveals that mitochondria abnormalities in APPwt or APPswe cells are correlated with Aβ1-42 levels secreted in the media (ng/ml, measure by ELISA). (*B*) Representative confocal microscopic pictures of wild type M17 cells transiently co-transfected with empty vector, DsRed-Monomer tagged wild type APP or mutant APPswe, and mito-AcGFP, either in the presence or absence of BACE inhibitor IV. White, Tubulin; Red, DsRed-Monomer; Green, mito-AcGFP; Blue, DAPI. (Scale bars, 10 μm.) (*C* and *D*) Quantitative analysis revealed that BACE inhibitor IV prevents APP-induced increase in abnormal mitochondria morphology (*C*) and distribution (*D*) (*, $P < 0.05$).

Fig. S4. Correlations between DLP1 (*A*), OPA1 (*B*), and Fis1 (*C*) with $A\beta_{1-42}$ level (ng/ml, measured by ELISA)/mitochondria distribution pattern/mitochondria fragmentation. Representative immunoblot (*D*) of DLP1/OPA1/Fis1 levels in APPswe cells (APPswe) and control neuroblastoma M17 cells (Control) demonstrated that BACE inhibitor abolished APP-induced changes in the levels of these proteins. Tubulin was used as internal control.

Fig. S5. Effects of DLP1, OPA1 and Fis1 on APP-induced mitochondrial abnormalities. APPwt or APPswe M17 cells were transiently cotransfected with myc-tagged DLP1, OPA1 or GFP-tagged Fis1 miR RNAi and mito-DsRed2. Representative confocal pictures (*A*) and quantification analysis (*B* and *C*) revealed that, in APPwt and APPswe cells, transient overexpression of DLP1 or OPA1 had differential effects but Fis1 knockdown has no effect on mitochondria morphology (*B*) and distribution (*C*) (*, $P < 0.05$, student t-test). White, Tubulin staining; Green, Myc staining or GFP; Red, mito-DsRed2; Blue, DAPI. (Scale bars, 10 μm.)

Fig. S6. (*A*) Representative immunoblot of Fis1 confirmed reduced expression of Fis1 in APPswe M17 cells transiently transfected with GFP-tagged miR RNAi expression vector targeted to Fis1. (*B* and *C*) Effects of DLP1 and OPA1 on APP-induced differentiation deficiency upon RA treatment. (*B*) Representative immunoblot of DLP1/OPA1/APP in APPswe M17 cells either stably overexpressing DLP1 or OPA1. (*C*) Percent of neurite-bearing neurons is determined as an index for differentiation. After 1 month of RA treatment, compared with empty-vector transfected control (vector), APPwt M17 and APPswe M17 cells demonstrated differentiation deficiency. DLP1 overexpression, but not OPA1 overexpression, in APPswe M17 cells leads to restoration of RA-induced differentiation.

Fig. S7. Effects of DLP1 and OPA1 on APP expression-induced mitochondrial functional changes. Different lines of M17 cells were plated at approximately 50% confluence on six-well plates. Twenty-four hours after seeding, cells were transfected with indicated plasmids. Forty-eight hours after transfection, ROS, relative MMP, and ATP were measured as described in *Materials and Methods*. *A–C* show quantification of ROS, relative MMP, and ATP in indicated cell lines with different manipulation. ($^{*}P < 0.05$ vs. non-transfected or empty-vector transfected normal control cells; $^{\#}P < 0.05$ vs. control or empty-vector transfected cells within each cell line, Student *t* test.)

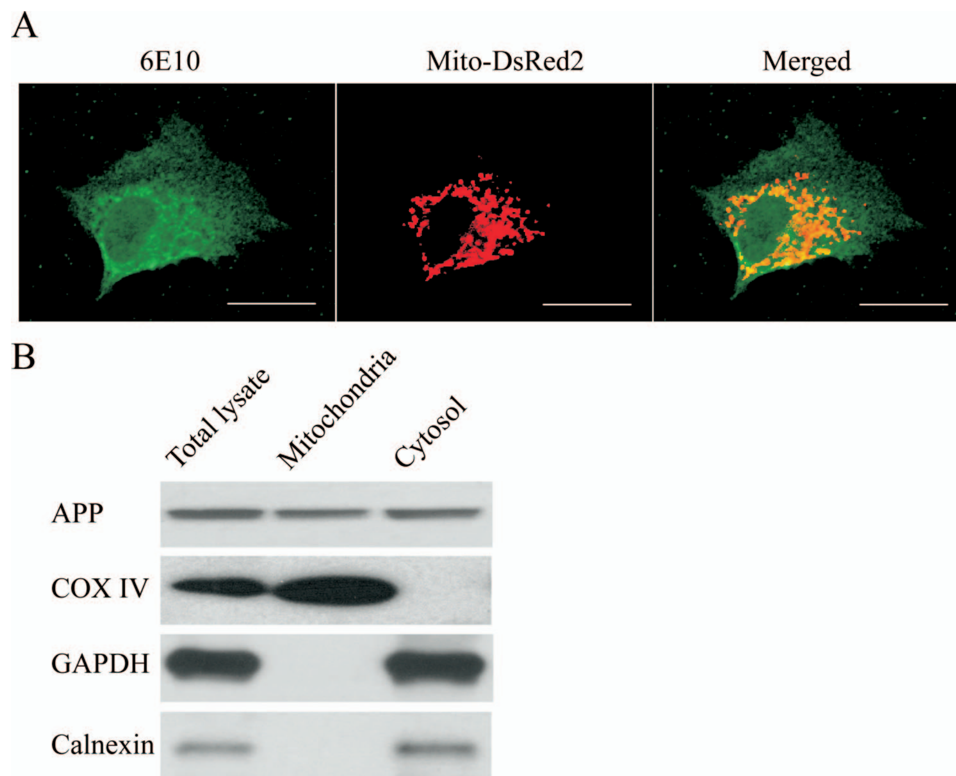

Fig. S8. Presence of APP in mitochondria in APPswe M17 cells. (*A*) APPswe cells were transfected with mito-DsRed2, fixed 2 days after transfection, and then stained with 6E10. Representative picture of positively transfected cells demonstrated co-localization between APP and mito-DsRed2 fluorescent signal. Red, DsRed; green, 6E10. (Scale bar, 20 μm.) (*B*) Immunoblot analysis confirmed the presence of APP in mitochondrial fraction prepared from APPswe M17 cell lysates. The cytosolic fraction contains all of the cellular compartments with the exception of nuclei and mitochondria. The purity of mitochondria fraction was confirmed by immunoblot detection of the mitochondria-specific marker cytochrome c oxidase IV, but not the endoplasmic reticulum-specific marker Calnexin and the cytosol-specific marker GAPDH in this fraction.

Fig. S9. It was reported that mitochondrial number is reduced but mitochondrial size is increased in AD (6 AD cases, 156 neurons) compared with control cases (5 control cases, 95 neurons) based on electron micrographs of cortical neurons from brain biopsy samples (Hirai *et al.,* 2001). This same set of electron micrographs (gift from George Perry and Mark A. Smith, Case Western Reserve University) was re-analyzed for lengths perpendicular to cristae of intact mitochondria. AD cases had significantly shorter mitochondria ($P < 0.05$, Student's t-test). Points represent the mean length for each case, and the lines the mean for each group (AD and control).